# 激光功率对激光－双丝脉冲MIG复合焊接电弧形态及熔滴过渡的影响

张晓枫[1]， 李 桓[1]， 杨立军[1]， 高 莹[2]
(1. 天津大学 天津市现代连接技术重点实验室，天津 300072;
2. 天津职业技术师范大学 天津市高速切削与精密加工重点实验室，天津 300222)

**摘 要**：通过搭建激光－双丝脉冲MIG复合焊接系统，利用高速摄像与电信号采集系统对激光－双丝脉冲MIG复合焊接在不同激光功率下的电压电流信号及高速摄像信号进行同步采集，研究激光功率对焊接过程的电弧形态、熔滴过渡过程的影响. 结果发现，由于激光等离子体与电弧等离子体的相互作用，电弧形态和熔滴受力状态发生改变. 随着激光功率的增大，激光对电弧的吸引能力增强，促进熔滴过渡的等离子流力竖直向下的分力减小，熔滴过渡频率降低.

**关键词**：激光－双丝脉冲MIG复合焊；熔滴过渡；电弧形态；高速摄像
**中图分类号**：TG 403 **文献标识码**：A **文章编号**：0253－360X(2014)11－0023－04

## 0 序 言

激光－双丝脉冲MIG复合焊接是将激光焊与双丝脉冲MIG焊结合到一起的焊接工艺，它综合了激光焊和电弧焊各自的特点，不仅具有激光焊接中焊接速度快、接头性能好等优点，而且继承了电弧焊接中桥接能力强、对工件定位要求低等优点. 同时由于激光与电弧的相互作用，激光诱导电弧增加了电弧能量密度，而电弧预热母材增加了激光吸收率. 激光电弧复合热源焊接方法被开发出来之后，国内外研究的精力主要集中在激光－TIG复合上，对激光－MIG/MAG复合研究较少[1,2]. 由于激光－双丝脉冲MIG复合焊接过程中有填充金属的熔化，且两电弧之间存在相互作用，电弧形态的变化较为剧烈，焊接过程更为复杂，所以开展激光－双丝脉冲MIG复合焊的研究对完善其工艺理论具有重要意义[3－5].

文中通过搭建激光－双丝脉冲MIG复合焊接试验系统，在焊接过程中改变激光功率研究光致等离子体与电弧等离子体间的相互作用，以及其对电弧形态和熔滴过渡过程的影响.

**收稿日期**：2013－05－10
**基金项目**：国家自然科学基金项目(51175374)；天津市应用基础及前沿技术研究计划项目(09JCYBJC05000)；天津市科技支撑计划重点项目(10ZCKFSF00200)

## 1 试验系统及焊接试验

激光－双丝脉冲MIG复合焊接试验系统由焊接系统和信号采集系统两部分组成. 如图1所示，焊接系统包括天津大学自行研制的MK03型脉冲控制器，林肯INVERTEC V350 PRO型弧焊电源(置于左侧)、林肯INVERTEC™ V300-I型弧焊电源(置于右侧)，两台S-86A型送丝机和英国GSI公司生产的JK2003SM型Nd:YAG激光器，其最大输出功率为2 kW，输出波长为1 064 nm的连续激光，焦距为300 mm，焦点半径为0.4 mm. 信号采集系统主要包括FASTCAM Super 10KC高速摄像机、电压传感器、电流传感器、数据采集卡(PCL-1742)、计算机及其附

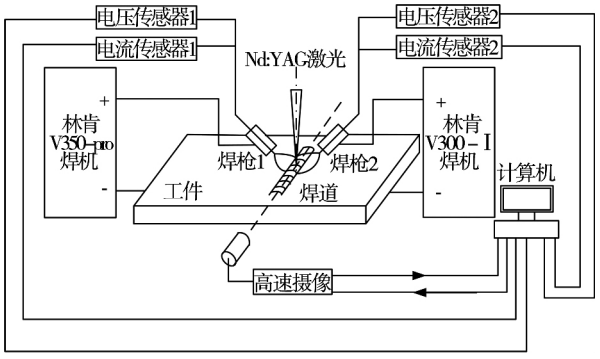


图1 激光－双丝脉冲MIG焊接系统示意图

Fig. 1 Schematic diagram of laser-twin-wire pulse MIG hybrid welding system

件. 焊接过程中高速摄像的采集频率为 1000 幅/s，电信号的采样频率为 10 kHz，可以实现焊接过程中电信号与高速摄像图片信号的同步采集.

试验中的两焊枪所在平面与焊接方向垂直，焊枪与工件的夹角均为 60°，左侧电弧由 V350 PRO 型弧焊电源供电，右侧电弧由 V300-I 型弧焊电源供电，均采用直流反接的形式. 其中 V350 PRO 型弧焊电源的输出形式为脉冲模式，V300-I 型弧焊电源在无外部控制时的输出形式为恒压模式. 在测量左侧焊接电流的电流传感器 1 处取出信号交由脉冲控制器进行处理，再由脉冲控制器控制 V300-I 型弧焊电源的电压呈脉冲式输出，当送丝速度不变时其焊接电流也呈脉冲式输出，两个电弧对应的脉冲电流具有一定的相位差[6]. 试验所用试板为 8 mm 厚的 Q235 低碳钢板. 焊丝为 H08Mn2SiA，直径 1.2 mm，两瓶保护气体均为纯氩气，气体流量均为 20 L/min，具体试验参数如表 1 所示.

表 1 试验参数

Table 1 Experimental parameters

| V350 预设值 $U_a$/V | V300 预设值 $U_b$/V | 激光功率 $P$/W | 送丝速度 $v_f$/(m·min$^{-1}$) | 焊接速度 $v_w$/(mm·s$^{-1}$) | 双丝间距 $L$/mm |
|---|---|---|---|---|---|
| 160 AMPS | 峰值 40.7<br>基值 23.1 | 0 ~ 1 500 | 3.0 | 5.0 | 7.0 |

## 2 试验结果与分析

### 2.1 激光功率对电弧形态的影响

双丝脉冲 MIG 焊中存在两个电弧等离子体，而在复合焊接中，激光的加入会产生光致等离子体. 光致等离子体与两个电弧等离子体三者之间存在复杂的相互作用，光致等离子体的出现使工件表面的等离子体浓度增加，引弧电阻降低. 同时由于激光作用产生的金属蒸气和小孔周围的高温等离子体为电弧提供了一个稳定的阴极斑点，能够引导电弧的弧柱，而导致电弧偏向激光作用区域的小孔处，使电弧能量更加集中，电弧的电流密度增加. 激光功率的改变可以影响光致等离子体的大小与强度，焊接温度场，熔滴表面张力以及两个电弧之间的相互作用力等[7,8].

图 2 分别为不同激光功率下左侧电流峰值，中间态(即两电弧形态大致相同的状态)及右侧电流峰值时的高速摄像. 如图 2 所示，激光功率为 0 W 时，左侧电流峰值时及右侧电流为峰值时，两个电弧均沿着焊丝轴线方向分布，中间态时两个电弧相互吸引，向中间偏移. 加入激光后，左侧电流峰值与左侧电流峰值时电弧均向激光入射方向偏移，中间态时两电弧的偏移角度增大. 由于 V350 焊机的峰值电流可达 420 A，V300 焊机的峰值电流约为 300 A，因此 V350 电弧的挺度高于 V300 的电弧，V350 电弧偏移程度相对较小. 当激光功率增大至 1 500 W 时，中间态及右侧电弧峰值状态下的激光入射处上方的光致等离子体与电弧等离子体发生强烈复合，激光对电弧产生明显的吸引作用. 由图 2 可知，激光对电弧的吸引能力及电弧偏向激光入射方向的角度随激光功率的提升而增大.

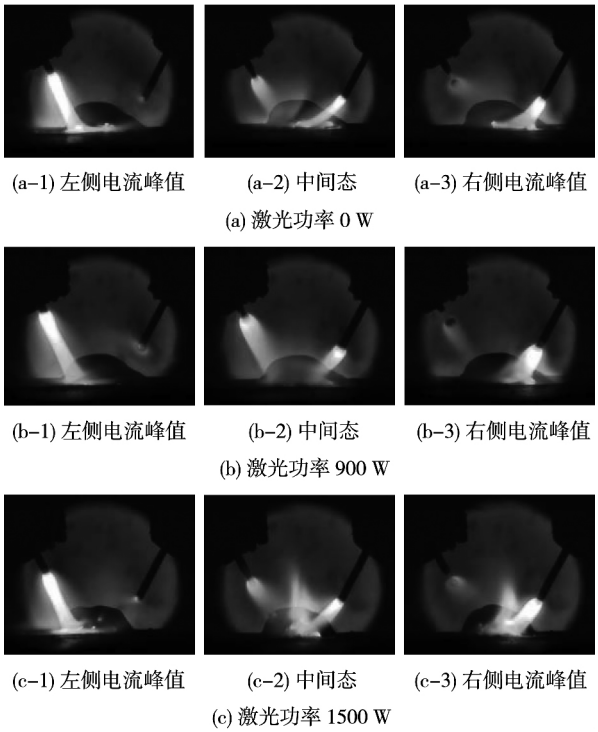


图 2 不同激光功率下的电弧形态

Fig. 2 Arc shape with different laser power

### 2.2 激光功率对熔滴过渡的影响

将焊接过程中采集的电压电流信号及与之同步的高速摄像图片进行处理，绘制出不同激光功率下熔滴过渡过程的电压电流信号与高速摄像的对应图.

图 3 为激光功率 $P=0$ W 时的电信号与高速摄像的对应图. 如图 3 所示，在 2.595 s 时，两个脉冲电流均处于基值阶段，电流较小，两个刚从焊丝脱落的熔滴即将进入熔池. 在 2.600 s 时左侧电流达到峰值，此后左侧电流下降，而右侧电流上升，在 2.603 s 时左侧电流已回到基值，右侧电流达到峰值，此过程中左侧焊丝的端部形成熔滴并脱离焊丝进入熔池，完成了一个一脉一滴的过渡过程. 在 2.608 s 时，左侧电流与右侧电流均位于基值，此时右侧焊丝的端部有熔滴存在，未完成过渡.

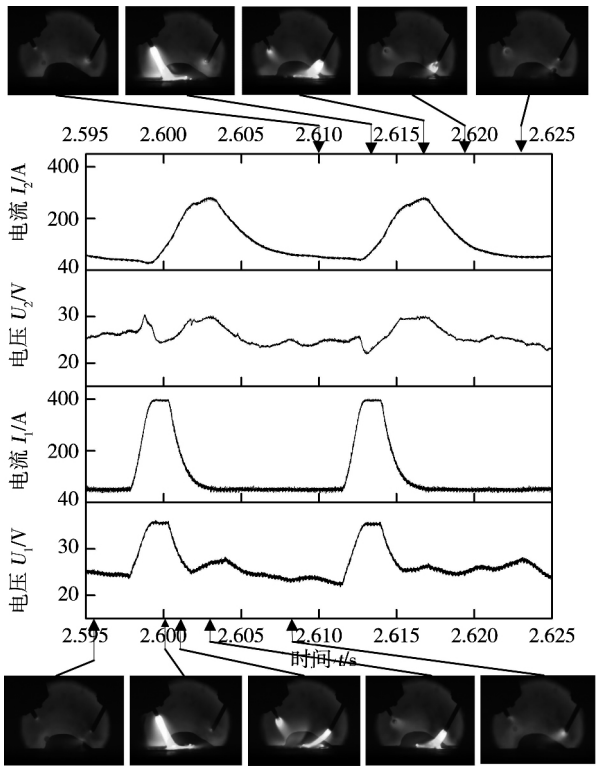


**图 3　激光功率 0 W 时一个熔滴过渡周期内的电信号及对应的高速摄像**

Fig. 3　High speed camera pictures and corresponding electrical signal in droplet transfer period when $P$ = 0 W

在时间 2.613 s 时左侧电流再次达到峰值，熔滴不断长大，随即液态熔滴完成颈缩，脱离焊丝. 2.617 s 时右侧电流达到峰值，前一脉冲周期内未脱离焊丝的熔滴继续长大，随即完成颈缩脱离焊丝，完成一个两脉一滴的熔滴过渡过程. 至 2.623 s 时，两个脉冲电流均位于基值.

图 4 为激光功率 1 500 W 时的电信号与高速摄像的对应图. 如图 4 所示，在 2.635 s 时，两个脉冲电流均处于基值阶段，电流较小，两个刚从焊丝脱落的熔滴即将进入熔池. 在 2.639 s 时左侧电流达到峰值，此后左侧电流下降，而右侧电流上升，在 2.643 s 时左侧电流回到基值，右侧电流达到峰值，此过程中左侧焊丝的端部形成熔滴，但未脱落，右侧焊丝端部的熔滴逐渐长大. 在 2.646 s 时，右侧电流回到基值，此时左侧焊丝与右侧焊丝的端部均有未脱落的熔滴存在. 2.653 s 时左侧电流达到峰值，熔滴继续长大，2.656 s 时左侧焊丝端部的熔滴完成颈缩，脱离焊丝，完成了一个两脉一滴的熔滴的过渡过程.

至 2.658 s 时右侧焊丝端部已形成了体积较大的熔滴，但仍未脱离焊丝. 至 2.667 s 时左侧达到峰值，焊丝端部再次形成熔滴，2.669 s 时左侧电流即

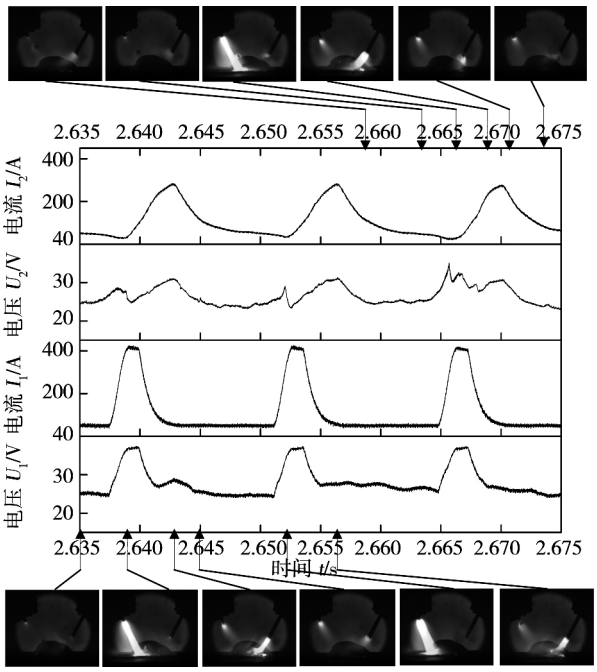


**图 4　激光功率 1 500 W 时一个熔滴过渡周期内的电信号及相对应的高速摄像**

Fig. 4　High speed camera pictures and corresponding electrical signal in droplet transfer period when $P$ = 1 500 W

将回到基值，对应的熔滴未脱离焊丝，此时右侧电流达到峰值，对应的熔滴不断长大. 2.671 s 时右侧焊丝端部的熔滴完成颈缩，脱离焊丝，完成了一个三脉一滴的熔滴的过渡过程. 至 2.674 s 时，两个脉冲电流均回到基值.

通过激光功率 0 W 与 1 500 W 时的熔滴过渡过程的对比可知，左侧弧焊电源对应的熔滴过渡形式由 $P$ = 0 W 时的一脉一滴变为 $P$ = 1 500 W 时的两脉一滴；右侧弧焊电源对应的熔滴过渡形式由 $P$ = 0 W 时的两脉一滴变为 $P$ = 1 500 W 时的三脉一滴. 两个弧焊电源对应的熔滴体积均有增大.

图 5 为复合焊接中激光功率与熔滴过渡频率对

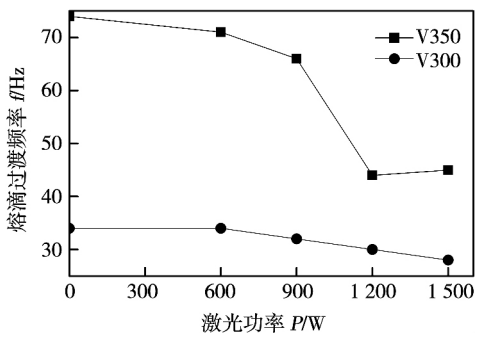


**图 5　不同激光功率下的熔滴过渡频率**

Fig. 5　Droplet transfer frequency with different laser power

应关系图. 如图 5 所示，随着激光功率的不断增大，左侧弧焊电源与右侧弧焊电源对应的熔滴过渡频率均不断降低. 其中左侧弧焊电源对应的熔滴过渡频率由 $P=0$ W 时的 74 Hz 降至 $P=1\ 500$ W 时的 45 Hz，降幅为 39.2%；右侧弧焊电源对应的熔滴过渡频率由激光功率 $P=0$ W 时的 34 Hz 降至 $P=1\ 500$ W 时的 28 Hz，降幅为 17.6%，二者相比左侧弧焊电源对应的变化幅度更为明显.

## 3 激光对熔滴过渡的影响机理分析

图 6 为激光 - 双丝脉冲 MIG 复合焊接过程中熔滴受力示意图. 其中 $F_g$ 为重力，$F_p$ 为等离子流力，$F_a$ 为两电弧之间的吸引力，$F_l$ 为激光对电弧的吸引力. 试验中焊接方式为平板堆焊，因此熔滴所受重力 $F_g$ 及等离子流力 $F_p$ 在竖直方向上的分力为促进熔滴过渡的力. 熔滴所受重力由熔滴自身质量决定，而等离子流力与焊接电流大小与电弧形态有关[9]. 在激光 - 双丝脉冲 MIG 复合焊接过程中，激光吸引电弧，使得两个电弧的等离子流力均向激光方向偏移，激光功率越大，吸引作用越强，电弧向激光入射方向的偏移越严重，等离子流力与竖直方向的夹角 $\theta$ 越大.

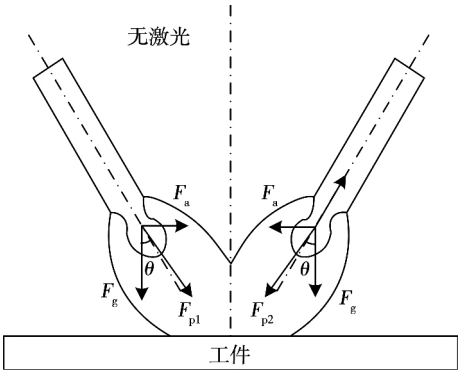


(a) 无激光时熔滴受力示意图

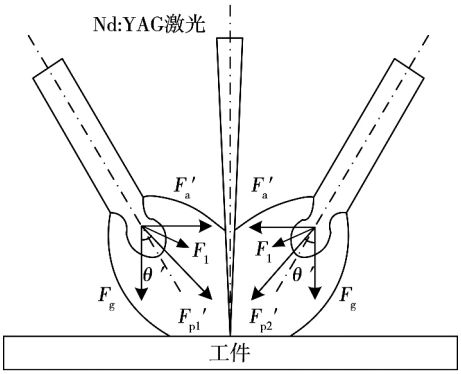


(b) 加入激光时熔滴受力示意图

图 6 激光 - 双丝脉冲 MIG 焊熔滴受力示意图

Fig. 6 Mechanical model of droplet in laser-twin-wire pulsed MIG hybrid welding

如图 6a 所示，未加入激光时，两个电弧对应的等离子流力 $F_{p1}$ 和 $F_{p2}$ 与竖直方向的分别夹角为 $\theta_1$ 和 $\theta_2$，力的大小值由焊接电流大小决定，左侧电流的峰值约为 450 A，右侧电流的峰值约为 300 A. 熔滴重力分别为 $F_{g1}$ 与 $F_{g2}$，两电弧之间的吸引力为 $F_a$. 此时的左侧弧焊电源对应的熔滴过渡形式为一脉一滴，右侧弧焊电源对应的为两脉一滴.

图 6b 为加入激光之后的熔滴受力示意图，其中电弧被激光吸引，等离子流力与竖直方向的夹角 $\theta$ 增大，促进熔滴过渡的力减小. 此时若熔滴的重力保持不变，则熔滴过渡不能顺利完成，下一个脉冲周期内熔滴继续长大，当熔滴所受重力与等离子流力分力的合力超过临界值时，熔滴过渡可顺利进行. 激光加入后，熔滴体积增大，所受重力增大，当激光功率逐渐增大时，激光对电弧的吸引能力增强，等离子流力与竖直方向的夹角增大，促进熔滴过渡的力减小，熔滴过渡频率降低. 当激光功率升至 1 500 W 时，左侧弧焊电源对应的熔滴过渡形式变为两脉一滴，右侧弧焊电源对应的变为三脉一滴.

## 4 结 论

(1) 激光 - 双丝脉冲 MIG 复合焊接中，激光功率的改变可以影响光致等离子体与两个电弧等离子体之间的相互作用，熔滴受力情况发生变化，从而影响电弧形态及熔滴过渡.

(2) 在焊接电源预设参数不变的情况下，光致等离子体与电弧等离子体之间的相互作用随激光功率的增大而不断增强. 左侧弧焊电源对应的熔滴过渡形式由均匀的一脉一滴变为两脉一滴，右侧弧焊电源对应的熔滴过渡形式由均匀的两脉一滴变为三脉一滴. 两台弧焊电源对应的熔滴过渡频率均随激光功率的增大而不断降低.

(3) 激光 - 双丝脉冲 MIG 复合焊中激光对电弧产生了明显的吸引作用，使熔滴受力情况发生改变，等离子流力向激光方向偏移，导致促进熔滴过渡的分力减小，使熔滴过渡更依赖于自身的重力作用，导致熔滴尺寸增大，过渡频率降低.

**参考文献:**

[1] 肖荣诗，吴世凯. 激光 - 电弧复合焊接的研究进展[J]. 中国激光，2008，35(11)：1680 - 1685.
Xiao Rongshi，Wu Shikai. Powgress on laser-arc hybrid welding [J]. Chin Journal Laser，2008，35(11)：1680 - 1685.

[下转第 62 页]

crashing and fatigue performance of high strength steels for automotive compnents [R]. SAE 2002 World Congress & Exhibition, 2002.

[2] 石 玗, 何翠翠, 黄健康, 等. 几种铝钢异种金属熔钎焊工艺的对比与分析 [J]. 焊接学报, 2014, 35(5): 1 - 4.
Shi Yu, He Cuicui, Huang jiankang, *et al*. Comparison and analysis on dissimilar metals welding of aluminum alloy to galvanized steel by different welding-brazing methods [J]. Transactions of the China Welding Institution, 2014, 35(5): 1 - 4.

[3] 杨 阳, 石 岩. 铝和钢异种金属焊接发展现状 [J]. 长春大学学报, 2011, 21(2): 21 - 25.
Yang yang, shi Yan. The development status of aluminum and steel dissimilar metal welding [J]. Journal of Changchun University, 2011, 21(2): 21 - 25.

[4] Qikawa H, Ohmiya S, Yoshimura T, *et al*. Resistance spot welding of steel and aluminum sheet using insert metal sheet [J]. Science and Technology of Welding & Joining, 1999, 4(2): 80 - 88.

[5] 邱然锋, 石红信, 张柯柯. 汽车车身用铝合金与钢的异种材料电阻点焊技术研究现状 [J]. 电焊机, 2012, 40(5): 150 - 153.
Qiu Ranfeng, Shi Hongxin, Zhang Keke. The current research status of resistance spot welding of aluminum alloy and steel for automobile body [J]. Electric Welding Machine, 2012, 40(5): 150 - 153.

[6] 秦红珊, 杨新岐. 一种代替传统电阻电焊的创新技术 - 搅拌摩擦点焊 [J]. 电焊机, 2006, 36(7): 27 - 30.
Qin Hongshan, Yang Xinqi. An alternative to the innovation of the traditional resistance welding technology-friction stir spot welding [J]. Electric Welding Machine, 2006, 36(7): 27 - 30.

[7] 王联凤, 朱小刚, 乔凤斌, 等. Al-Mg 合金填充式搅拌摩擦点焊性能 [J]. 焊接学报, 2014, 35(2): 99 - 103.
Wang Lianfeng, Zhu Xiaogang, Qiao Fengbin, *et al*. Properties of Al-Mg alloys joints welded by refill friction stir spot weldeing process [J]. Transactions of the China Welding Institution, 2014, 35(2): 99 - 103.

[8] Pan T, Joaquin A, Wilkosz D E, *et al*. Spot friction welding for sheet aluminum joining, proc [C] // 5th International Symposium on Friction Stir Welding, Metz, France, 2004.

[9] 雷 振, 秦国梁, 林尚扬, 等. 铝与钢异种金属焊接的研究与发展概况 [J]. 焊接, 2006(4): 16 - 20.
Lei Zhen, Qin Guoliang, Lin Shangyang, *et al*. The research and development situation of dissimilar metal welding of aluminum and steel [J]. Welding & Joining, 2006(4): 16 - 20.

[10] 傅 莉, 毛信孚, 史学芳. LF6 防锈铝与 HR-2 抗氢不锈钢摩擦焊接 [J]. 焊接学报, 2003, 24(1): 9 - 14.
fu Li, Mao Xinfu, Shi Xuefang. LF6 aluminum antirust and HR-2 hydrogen resistant stainless steel friction welding [J]. Transactions of the China Welding Institution, 2003, 24(1): 9 - 14.

[11] 李永兵, 魏泽宇, 雷海洋, 等. 基于 CMT 的铝合金电弧点焊方法及焊接系统 [P]. 中国: CN102896398 A, 2013 - 01 - 30.

[12] GB/T 15111—1994, 点焊接头剪切拉伸疲劳试验方法 [S]. 北京: 中国标准出版社, 1994.

**作者简介:** 黄 倩, 女, 1987 年出生, 硕士研究生. 主要从事异种金属的焊接性研究. 发表论文 1 篇. Email: qian110327@163.com

**通讯作者:** 曹 睿, 女, 教授, 博士研究生导师. Email: caorui@lut.cn

[上接第 26 页]

[2] Claus E, Marc K, Nikolai P. Development of plasma-laser hybrid welding process [J]. Physics Procedia, 2011(12): 194 - 200.

[3] 吴艳明, 王 威, 林尚扬, 等. Nd:YAG 激光 - 脉冲 MAG 复合热源焊熔滴过渡分析 [J]. 焊接学报, 2011, 32(7): 83 - 86.
Wu Yanming, Wang Wei, Lin Shangyang, *et al*. Analysis of droplet behavior in Nd: YAG laser-pulsed MAG hybrid welding [J]. Transactions of the China Welding Institution, 2011, 32(7): 83 - 86.

[4] 武传松, 胥国祥, 秦国梁, 等. 电弧功率对 Laser + GMAW-P 复合热源焊热场特征的影响 [J]. 金属学报, 2009, 45(8): 1000 - 1005.
Wu Chuansong, Xu Guoxiang, Qin Guoliang, *et al*. Effect of arc power on theamal field characteristics of laser + GMAW-P hybid welding [J]. Acta Metall Sin, 2009, 45(8): 1000 - 1005.

[5] El Rayes M, Walz C, Sepold G. The influence of various hybrid welding parameters on bead geometry [J]. Welding Journal, 2004, 83(5): 147 - 153.

[6] 李 桓, 王 莉, 杨 倩, 等. 林肯 V300-I 焊机脉冲焊功能的开发与实现 [J]. 电焊机, 2005, 35(12): 9 - 11.
Li Huan, Wang Li, Yang Qian, *et al*. Development of pulsed welding performance on lincoln INVERTEC V300-I [J]. Electric Weld Machine, 2005, 35(12): 9 - 11.

[7] 韦辉亮, 李 桓, 王旭友, 等. 激光 - MIG 电弧的复合作用及对熔滴过渡的影响 [J]. 焊接学报, 2011, 32(11): 41 - 44.
Wei Huiliang, Li Huan, Wang Xuyou, *et al*. Hybrid interaction of laser and pulsed MIG arc and its influence on metal transfer [J]. Transactions of the China Welding Institution, 2011, 32(11): 41 - 44.

[8] Li K H, Wu C S. Mechanism of metal transfer in DE-GMAW [J]. Journal of Material Science and Technology, 2009, 25(3): 415 - 418.

[9] 贾昌申, 肖克民, 殷咸青, 等. 焊接电弧的等离子流力 [J]. 焊接学报, 1994, 15(2): 101 - 105.
Jia Changshen, Xiao Kemin, Yin Xianqing, *et al*. Plasma flow force of welding arc [J]. Transactions of the China Welding Institution, 1994, 15(2): 101 - 105.

**作者简介:** 张晓枫, 男, 1989 年出生, 硕士研究生. 研究方向为激光 + MIG/MAG 复合焊接. Email: zxf@tju.edu.cn

**通讯作者:** 杨立军, 男, 副教授. Email: yljabc@tju.edu.cn

crack initiation and propagation of welded joint, finite element method was used to calculate the stress concentration and stress intensity factor around the pores. Finally, the characteristics of fatigue crack initiation and propagation with welding defects were discussed.

**Key words:** welded joint; aluminium alloy; super high cycle fatigue; pore; stress intensity factor

**Effect of laser power on arc behavior and metal transfer in laser-twin-wire pulsed MIG hybrid welding process**

ZHANG Xiaofeng[1], LI Huan[1], YANG Lijun[1], GAO Ying[2] (1. Tianjin Key Laboratory of Joining Technology, Tianjin University, Tianjin 300072, China; 2. Tianjin Key Laboratory of High-speed Cutting & Precision Machining, Tianjin Vocational and Technical Normal University, Tianjin 300222, China). pp 23 - 26, 62

**Abstract:** Laser-twin-wire pulsed MIG hybrid welding is a new welding technology which combines laser welding and twin-wire MIG welding. As one of the most important factors in this technology, laser power has significant effect on the welding procedure and properties of joint. A laser-twin-wire pulsed MIG hybrid welding system was established to investigate the effect of laser power on arc behavior and metal transfer in this process. High-speed photography system with synchronous electrical signal, including current and voltage signals, were adopted to record the arc behavior and metal transfer during welding. The results showed that the arc shape and stress status of the droplet were affected by the interaction between laser-induced plasma and arc plasma. With the increase of laser power, the laser-arc attraction was enhanced, the component force of plasma stream force in the vertical downward which could promote droplet transfer reduced. As a result, the droplet transfer frequency decreased.

**Key words:** laser-twin-wire pulsed MIG hybrid welding; metal transfer; arc behavior; high-speed photography

**Morphology of molten pool based on shadow during high-power laser deep penetration welding**

ZHANG Yanxi, GAO Xiangdong (School of Electromechanical Engineering, Guangdong University of Technology, Guangzhou 510006, China). pp 27 - 30

**Abstract:** The morphology of molten pool, especially the volume of molten pool can not be measured directly by the current measurement methods. In this study, surfacing welding of thick 304 stainless steel plate with high-power disk laser welding was conducted. With extra auxiliary infrared laser light and high-speed camera, clear images of the molten pools and their shadows were obtained, and then the shadow area of molten pool was extracted to be analyzed by one-dimensional linear regression equation and correlation coefficient analysis method. The experimental results confirmed that the shadow area variation of molten pool had positive correlation with welding quality, and this provided a new method for test of welding quality.

**Key words:** high-power disk laser welding; shadow of molten pool; morphology of molten pool; welding quality

**Activating brazing of Gr/2024Al composite material to TC4 titanium alloy with Ag-Cu-Sn-Ti filler**

SHI Junmiao[1], ZHANG Lixia[1], LI Hongwei[1], TIAN Xiaoyu[1], FENG Jicai[1,2] (1. State Key Laboratory of Advanced Welding and Joining, Harbin Institute of Technology, Harbin 150001, China; 2. Shandong Provincial Key Laboratory of Special Welding Technology, Harbin Institute of Technology, Weihai 264209, China). pp 31 - 34, 38

**Abstract:** Gr/2024Al composite material and TC4 titanium alloy were successfully brazed with self-developed Ag-Cu-Sn-Ti filler alloy, and the interfacial microstructure and mechanical properties of the brazed joints were investigated. The results show that the typical interfacial structure of brazed joint was Gr/2024Al composite material/$Ti_3AlC_2$/$Ag_2Al$ + $Ag_3Sn$ + $Al_2Cu$ + $Al_5CuTi_2$/$Al_5CuTi_2$/$TC_4$ titanium alloy. With the increasing of brazing temperature and extending of dwelling time, the amount of Al2Cu compounds decreased but the amount of $Al_5CuTi_2$ increased and it finally grew into bulk in the brazed seam. While brazed at 953 K for 10 min, the joint obtained maximum shear strength of 17 MPa at room temperature.

**Key words:** Gr/2024Al composite material; TC4; Ag-Cu-Sn-Ti filler; interfacial microstructure; shear strength

**Weldability of dissimilar steels for high-end cutting tools with A-TIG welding**

YIN Yan[1], LIU Zhao[1], SUN Peng[1], ZHANG Ruihua[2], LI Jihui[3] (1. State Key Laboratory of Gansu Advanced Non-ferrous Metal Materials, Lanzhou University of Technology, Lanzhou 730050, China; 2. China Iron & Steel Research Institute Group, Beijing 100081, China; 3. Yang Jiang ShiBaZi Group, Yangjiang 529500, China). pp 35 - 38

**Abstract:** In TIG welding of high-end cutting tools, the entire tools must be preheated. A-TIG welding was selected in this paper to weld 430 stainless steel knife back and sandwich (3Cr13-1Cr17-3Cr13) stainless steel blade, and study the effect of fluxes on the weld shape. The differences between A-TIG and conventional TIG on the weld penetration, pores in the weld, microstructure, mechanical properties and corrosion resistance of the joint were studied in this paper. The results show that satisfied joint with excellent weld appearance between 430 stainless steel knife back and sandwich (3Cr13-1Cr17-3Cr13) stainless steel blade could be achieved by A-TIG welding. No defects were detected in the joint and the grains in weld were refined. The HAZ was very narrow and the tensile strength of joint was 606 MPa. The activating flux did not reduce the corrosion resistance of welded joint.

**Key words:** A-TIG welding; dissimilar steels; microstructure; mechanical property

**Effect of detonation velocity on interface and properties of Al/Ti composite tube under explosive welding**

DENG Wei[1,2], LU Ming[2], XU Qian[2] (1. 63981 Unite of PLA, Wuhan 430311, China; 2. College of Field Engineering, PLA Univ. of Sci. & Tech., Nanjing 210007, China). pp 39 - 42

**Abstract:** To obtain low detonation velocity explosive, commercial attenuant was blended into the emulsion explosive.